Talanta 155 (2016) 336–346

Contents lists available at ScienceDirect

Talanta

journal homepage: www.elsevier.com/locate/talanta

In situ analysis of lipid oxidation in oilseed-based food products using near-infrared spectroscopy and chemometrics: The sunflower kernel paste (tahini) example

Vlad Mureșan [a,*], Sabine Danthine [b], Andruța Elena Mureșan [a], Emil Racolța [a], Christophe Blecker [b], Sevastița Muste [a], Carmen Socaciu [c], Vincent Baeten [d]

[a] Food Engineering Department, University of Agricultural Sciences and Veterinary Medicine Cluj-Napoca, 64 Calea Florești, 400509 Cluj-Napoca, Cluj, Romania
[b] Food Science and Formulation Department, Gembloux Agro-Bio Tech, University of Liège, 2 Passage des Déportés, 5030 Gembloux, Belgium
[c] Food Science Department, University of Agricultural Sciences and Veterinary Medicine Cluj-Napoca, 3-5 Calea Mănăștur, 400372 Cluj-Napoca, Cluj, Romania
[d] Valorisation of Agricultural Products Department, Walloon Agricultural Research Centre (CRA-W), 24 Henseval Building, Chaussée de Namur, 5030 Gembloux, Belgium

ARTICLE INFO

Article history:
Received 1 January 2016
Received in revised form
6 April 2016
Accepted 8 April 2016
Available online 8 April 2016

Keywords:
NIR method for lipid oxidation
In situ analysis
Peroxide and p-anisidine values
Nut spread oxidative stability
Oilseed oxidation
Particle size

ABSTRACT

A new near-infrared (NIR) spectroscopic method was developed for the analytical measurement of lipid oxidation in sunflower kernel paste (tahini), which was chosen as an example of a complex oilseed-based food product. The NIR spectra of sunflower tahini were acquired for the extracted fat phase (EFP) and for the intact sunflower tahini (IST) samples during controlled storage. The best peroxide value (PV) calibration models were considered suitable for quality control (ratio of performance of deviation [RPD] > 5). The best PV partial least squares (PLS) model result for EFP (RPD 6.36) was obtained when using standard normal variate (SNV) and the Savitzky-Golay first derivative in the 1140–1184 nm, 1388–1440 nm and 2026–2194 nm regions. In the case of IST spectra, the best PV models (RPD 5.23) were obtained when either multiple scattering correction (MSC) or SNV were followed by the Savitzky-Golay second derivative for the 1148–1180 nm and 2064–2132 nm regions. There were poor correlations between the NIR-predicted values and the reference data of the p-anisidine value (pAV) for both EFP and IST. Overall, the results obtained showed that NIR spectroscopy is an appropriate analytical tool for monitoring sunflower paste PV *in situ*. Due to the nonexistence of the extraction step, it demonstrates a unique and substantial advantage over presently known methods. Based on these results it is strongly recommended that, when using NIR PLS models to assess lipid oxidation *in situ* in similar oilseed-based food products (e.g., sesame tahini, hazelnut and cocoa liquor used for chocolate production, peanut butter, hazelnut, almond, pistachio spreads), suitable calibration sets containing samples of different particle sizes and stored at different temperatures be selected.

1. Introduction

Lipid oxidation analysis is an important issue in food quality assessment because the compounds generated are related to undesirable sensory and biological effects [1]. The control of lipid oxidation in food systems is therefore necessary to ensure high

Abbreviations: CoaT, coarse sunflower tahini; ComT, commercial sunflower tahini; CVP, cumulative volume percentages; d1/d2, first/second derivative; EFP, extracted fat phase; FinT, fine sunflower tahini; IST, intact sunflower tahini; LP, large particle size population; MIR, middle infrared; MP, middle particle size population; MSC, multiple scattering correction; NIR, near-Infrared; P, sunflower tahini particle size; pAV, p-anisidine value; PLS, partial least squares; PV, peroxide value; R_{cal}^2, R_{cv}^2, R_p^2, coefficients of determination for calibration, cross-validation and prediction; RMSEC, RMSECV, RMSEP, root mean square error of calibration, cross-validation and prediction; RPD, ratio of performance of deviation; RT, room temperature; SD, standard deviation; SEC, SECV, SEP, standard error of calibration, cross-validation and prediction; SNV, standard normal variate; SP, small particle size population; T, storage temperature; τ, storage time

* Corresponding author.
E-mail addresses: vlad.muresan@usamvcluj.ro (V. Mureșan), sabine.danthine@ulg.ac.be (S. Danthine), andruta.muresan@usamvcluj.ro (A.E. Mureșan), emil.racolta@usamvcluj.ro (E. Racolța), christophe.blecker@ulg.ac.be (C. Blecker), sevastita.muste@usamvcluj.ro (S. Muste), carmen.socaciu@usamvcluj.ro (C. Socaciu), v.baeten@cra.wallonie.be (V. Baeten).

http://dx.doi.org/10.1016/j.talanta.2016.04.019
0039-9140/

levels of quality and safety. Foods are highly complex and heterogeneous systems, composed mainly of water, carbohydrates, proteins and fats, as well as other constituents that are present at low concentrations, such as vitamins and minerals [2]. Lipid deterioration is characteristic of foods rich in fats, such as vegetable oil, lard, or butter-based products (*e.g.*, nut spreads, cookies, snacks, margarine, dressings). Due to their high oil content and their high proportion of polyunsaturated fatty acids, coupled with the thermal stress caused by roasting if used, oilseed-based products are more prone to lipid deterioration. Regardless of the oilseed raw material used (*e.g.*, peanuts, sesame, hazelnuts, almonds, sunflower, walnuts), the food products obtained display a complex chemical composition and are similar in their behavior and use. Sunflower kernels, for example, are consumed raw or roasted as snacks, as well as being used intact or milled in several food products, including bakery products [3], sunflower butter [4], halva (a confection that includes nougat and an oilseed paste) [5] and other value-added products [6]. When used for sunflower butter, halva, dressing or as an ingredient in new food formulations, usually the whole sunflower kernels are roasted and then milled into a paste called 'tahini'. Tahini is a word from Arabic طحينة [tˤaħiːna] that has the same root as طحين [tˤaħiːn], which means 'flour'. The term tahini is generally assigned to roasted sesame paste, but in Central Eastern Europe for many decades sesame seeds have been completely replaced by sunflower seeds, resulting in a cheaper product, roasted sunflower kernel paste (sunflower tahini). Given the chemical composition of sunflower kernels (20.4–40% protein, 47–65% lipids, 4–10% carbohydrates [7]), sunflower kernel tahini could be considered as a good example of a complex food matrix.

Like other oilseed-based products, after prolonged storage sunflower kernel tahini usually has a rancid flavor. Measuring the oxidative stability of oilseed-based food products is essential for determining their shelf life, consumer acceptability and nutritional quality. Oxidative stability index (OSI) is a well-known parameter to assess the oxidation status of lipids. However, the method is not suitable for whole oilseed based products while it involves the existence of a sample with very low viscosity in order to bubble the air into. However, if a prior extraction of the lipid phase is performed, the OSI might be determined also for extracted fat phase of complex foods, but higher analysis times and costs are involved. The peroxide value (PV) is most commonly used to assess oxidation in oils and food containing lipids, being applicable to the early stages of oxidation. In order to monitor accumulated secondary oxidation products, usually carbonyl-type compounds, the p-anisidine value (pAV) test is a widely used method [8]. Both methods, however, are time consuming, destructive and costly and they require large amounts of glassware, samples and potentially hazardous reagents. In addition, when assessing the oxidative status of a food matrix, a preliminary extraction of the fat phase is required. This step, alongside the supplementary manipulation and costs, can be the source of erroneous results. The increased industrialization and globalization of the food chain requires efficient analysis methods. New analytical solutions based on spectroscopic technologies are promising tools for food analysis, showing clear advantages such as speed, ease of use, reasonable start-up cost, non-destructiveness and the possibility of implementation online or directly in the field. The development of *in situ* methods that would not require the extraction step and would allow the direct quantification of the lipid oxidation of complex food products would greatly enhance the ability to assess the oxidation status of oilseed-based food products.

The possibility of measuring the oxidation status of intact food using *in situ* near-infrared (NIR) spectroscopy measurements has been studied for crackers and noodles [9] and for potato crisps [10]. Middle infrared (MIR) spectroscopy has been used for the oxidation index assessment of emulsions containing soybean and palm kernel oil [11]. The oil phase of these types of products, however, is either sprayed on the surface or present in very low quantities, or the products are very specific in terms of composition, thus limiting the extrapolation of the described methods for a larger group of oilseed-based products with more complex chemical compositions. In addition, the use of infrared methods for the *in situ* analysis of lipids in agro-food products applies mainly to the determination of fat content or fatty acid compositions. Studies have been conducted on intact cereals and feed [12], olives [13], oilseed rape [14], sesame [15], sunflower [16] and safflower [17]. So far as we know, there have not yet been any studies on the *in situ* infrared spectroscopic measurement of lipid oxidation in intact oilseeds or oilseed-based products. Several studies have focused on the development of methods for assessing oil and fat oxidation based on MIR [18,19] and NIR [20–23]. The application of handheld portable infrared spectrometer for monitoring oil oxidative stability [24] or for quantitation of trans fat in edible oils [25] were also reported. Although the NIR technique is being more frequently used in oil and fat quality control [26], its use in the *in situ* assessment of lipid oxidation has not been studied for oilseed-based food products, neither using bench-top or portable instruments.

This paper reports on a feasibility study initiated to assess the use of NIR spectroscopy for determining *in situ* the PV and pAV of sunflower kernel tahini, a heterogeneous and complex food model representative of the oilseed-based products category. In order to ensure model robustness, a broad range of degrees of oxidation was achieved using a controlled storage test. In addition, new NIR calibrations and validation strategies were developed using the various experimental factors relevant for food matrices: particle size, storage temperature and storage time. Since classical spectrophotometric measurements of oil and fats oxidation are well established and considered routine, the new analytical method proposed here for a complex food matrix demonstrates a unique and substantial advantage over presently known methods, due to the nonexistence of the extraction step, the analysis being performed on the product as it is ("*in situ*").

2. Materials and methods

2.1. Sunflower tahini preparation and particle size characterization

Sunflower tahini samples were prepared by controlling the milling process [27] of roasted sunflower kernels (total fat 60.07%; crude protein 20.55%; ash 3.87%; moisture 0.73%). The coarse sunflower tahini (CoaT) was obtained by a single passing of the kernels through a colloidal mill Microcut MCV 12B (Stephan Machinery GmbH, Hameln, Germany) and the fine sunflower tahini (FinT) was obtained by eight passes through the mill. A commercial sunflower tahini (ComT) obtained industrially via a two-step process, using a three-roll refiner and a beating machine (SC Amylon SA Sibiu, Romania), was also analyzed. As determined previously [27], the ComT particle size was in-between CoaT and FinT, all samples showing trimodal particle size distribution with the following particle size populations: small (SP) [$\sim$0.2 to $\sim$2 μm], middle (MP) [$\sim$2 to $\sim$60 μm] and large (LP) [> $\sim$60 μm]. The correspondent cumulative volume percentages (CVP) of each size class were: for CoaT, SP −9.61%, MP −43.03%, LP −47.36%; for FinT, SP −16.67%, MP −55.03%, LP −28.30%; and for ComT, SP −10.51%, MP −36.90%, LP −52.59%.

2.2. Fat extraction and peroxide and p-anisidine value determination

For all the samples, in order to avoid lipid supplementary oxidation, oil was extracted at low temperatures (< 40 °C), following the method described by Folch et al. [28]. The primary oxidation products were measured using a PV based on a small-scale modification of the AOCS Official Method Cd 8-53 described by Crowe and White [29]. Secondary oxidation products were measured by determining the pAV according to the AOCS Official Method Cd 18-90 [30]. The standard errors for the PV and pAV laboratory methods were 0.15 and 0.07, respectively.

2.3. NIR measurements

A Foss XDS (FOSS, Hillerød, Denmark) spectrophotometer was used to collect spectra with a resolution of 8 cm^{-1}, resulting in 32 co-added scans. All the spectra were recorded from 1100 nm to 2500 nm and processed with Winisi 4.0 software. The cell used was a gold cell MCRFL0.1 and duplicate measurement was done in transflectance mode. Data treatment and calibration models were performed using chemometric software (The Unscrambler v9.7; CAMO Software, Norway).

2.4. Management of NIR data

An ideal calibration set should cover the chemical and physical characteristics of the population being analyzed and avoid future extrapolations when predicting new samples. In order to create a wide range of degrees of oxidation for sunflower tahini, a controlled storage test was performed using three factors in the design: sunflower tahini particle size, storage temperature and storage time. Two of the factors had three levels, and one factor had six levels:

- sunflower tahini particle size (P): CoaT, FinT and ComT
- storage temperature (T): 4 ± 1 °C, 25 ± 3 °C (room temperature – RT) and 40 ± 1 °C
- storage time (τ): t1 = initial state, t2 = 5 days, t3 = 2 weeks, t4 = 1 month, t5 = 2 months and t6 = 3 months.

A total of 54 samples were obtained from the full factorial design (3 levels of factor P × 3 levels of factor T × 6 levels of factor $\tau = 54$). For clarity, in Table 1 the samples are represented as S(*x, y, z*), where *x, y* and *z* are the levels corresponding to sunflower tahini particle size, storage temperature and storage time, respectively. For example, S(CoaT, 4 °C, t4) refers to the coarse sunflower

Table 1
Peroxide and p-anisidine value descriptive statistics (mean, standard deviation and range) of the various calibration and external validation sets considered with set description (samples included, number of samples, percents).

Code	Samples included	Description	n	[%][e]	Mean	SD	Range
		I. Peroxide value [meq O_2 kg^{-1}]					
A. Calibration sets							
C1′	**S(x, y, z)**[a] | x∈P[b]; y ∈ T[c]; z ∈ τ[d]	All samples	54 (3 × 3 × 6)	100	38.57	23.88	8.42–125.21
C2′	**S(CoaT, y, z); S(FinT, y, z)** | y ∈ T; z ∈ τ	CoaT, FinT	36 (2 × 3 × 6)	66.7	45.70	22.85	21.34–125.21
C3′	**S(CoaT, y, z); S(ComT, y, z)** | y ∈ T; z ∈ τ	CoaT, ComT	36 (2 × 3 × 6)	66.7	30.79	20.95	8.42–100.12
C4′	**S(FinT, y, z); S(ComT, y, z)** | y ∈ T; z ∈ τ	FinT, ComT	36 (2 × 3 × 6)	66.7	39.23	25.21	8.42–125.21
C5′	**S(x, 4 °C, z); S(x, RT, z)** | x ∈ P; z ∈ τ	Stored at 4 °C and RT	36 (3 × 2 × 6)	66.7	32.23	14.94	8.42–72.79
C6′	**S(x, 4 °C, z); S(x, 40 °C, z)** | x ∈ P; z ∈ τ	Stored at 4 °C and 40 °C	36 (3 × 2 × 6)	66.7	40.43	26.77	8.42–125.21
C7′	**S(x, 40 °C, z); S(x, RT, z)** | x ∈ P; z ∈ τ	Stored at 40 °C and RT	36 (3 × 2 × 6)	66.7	43.06	26.86	8.42–125.21
C8′	**S(x, y, t1); S(x, y, t3); S(x, y, t4); S(x, y, t6)** | x ∈ P; y ∈ T	Storage times 1, 3, 4, 6	36 (3 × 3 × 4)	66.7	38.94	25.14	8.42–125.21
C9′	**S(x, y, t1); S(x, y, t2); S(x, y, t5); S(x, y, t6)** | x ∈ P; y ∈ T	Storage times 1, 2, 5, 6	36 (3 × 3 × 4)	66.7	41.28	27.21	8.42–125.21
C10′	Randomly selected[f]		42	77.8	39.70	25.29	8.42–125.21
B. External validation sets							
V2′	**S(ComT, y, z)** | y ∈ T; z ∈ τ	ComT	18 (1 × 3 × 6)	33.3	24.32	19.49	8.42–81.84
V3′	**S(FinT, y, z)** | y ∈ T; z ∈ τ	FinT	18 (1 × 3 × 6)	33.3	54.14	22.12	39.12–125.21
V4′	**S(CoaT, y, z)** | y ∈ T; z ∈ τ	CoaT	18 (1 × 3 × 6)	33.3	37.25	20.85	21.34–100.12
V5′	**S(x, 40 °C, z)** | x ∈ P; z ∈ τ	Stored at 40 °C	18 (3 × 1 × 6)	33.3	51.26	32.6	8.42–125.21
V6′	**S(x, RT, z)** | x ∈ P; z ∈ τ	Stored at RT	18 (3 × 1 × 6)	33.3	34.86	16.75	8.42–72.79
V7′	**S(x, 4 °C, z)** | x ∈ P; z ∈ τ	Stored at 4 °C	18 (3 × 1 × 6)	33.3	29.59	12.82	8.42–53.03
V8′	**S(x, y, t2); S(x, y, t5)** | x ∈ P; y ∈ T	Storage times 2, 5	18 (3 × 3 × 2)	33.3	37.85	21.81	10.92–84.50
V9′	**S(x, y, t3); S(x, y, t4)** | x ∈ P; y ∈ T	Storage times 3, 4	18 (3 × 3 × 2)	33.3	33.16	14.39	14.08–68.12
V10′	Randomly selected [f]		12	22.2	34.61	18.46	8.42–80.37
		II. p-anisidine value[g]					
A. Calibration sets							
C1″	**S(x, y, z)** | x ∈ P; y ∈ T; z ∈ τ	All samples	54	100	5.96	1.32	3.78–8.9
C2″	**S(x, 4 °C, z)** | x ∈ P; z ∈ τ	Stored at 4 °C	18 (3 × 1 × 6)	33.3	5.23	0.86	3.87–6.76
C3″	**S(x, RT, z)** | x ∈ P; z ∈ τ	Stored at RT	18 (3 × 1 × 6)	33.3	5.53	0.85	3.78–6.63
C4″	**S(x, 40 °C, z)** | x ∈ P; z ∈ τ	Stored at 40 °C	18 (3 × 1 × 6)	33.3	7.13	1.33	4.12–8.9

n = number of samples in the calibration/validation set; SD = standard deviation.

[a] samples were represented as S(*x, y, z*) where *x, y,* and *z* are the levels corresponding to experimental factors: sunflower tahini particle size, storage temperature, and storage time, respectively.

[b] sunflower tahini particle size P = {CoaT, ComT, FinT}, where CoaT, FinT, and ComT refer to fine, coarse and commercial sunflower tahini, respectively.

[c] storage temperature T = {4 °C, RT, 40 °C}, where RT is room temperature.

[d] storage time τ = {t1, t2, t3, t4, t5, t6}, where t1 is the initial state, t2 = 5 days, t3 = 2 weeks, t4 = 1 month, t5 = 2 months, t6 = 3 months.

[e] computed by taking into account the total number of samples (*i.e.*, 54).

[f] the samples selected for sets C10′ and V10′ were inspected to ensure a broad oxidation index range by covering all experimental factors. The set V10′ included the following samples: S(CoaT, 4 °C, t1), S(FinT, 40 °C, t1), S(ComT, RT, t1), S(CoaT, RT, t2), S(FinT, 4 °C, t2), S(ComT, 40 °C, t2), S(FinT, 4 °C, t3), S(CoaT, 40 °C, t4), S(ComT, RT, t4), S(CoaT, 40 °C, t5), S(CoaT, 4 °C, t6), S(ComT, RT, t6), whereas the set C10′ included the remaining 42 samples from the experimental design.

[g] no external validation sets were used for p-anisidine value.

tahini being stored at 4 °C for 1 month, whereas S(ComT, RT, t6) refers to the commercial sunflower tahini being stored at room temperature for 3 months. Different grouping strategies were used to obtain various calibration and validation sets, based on the experimental factors and their levels. The set code, the samples included (short description, number and percentage) and the PV and pAV statistics (mean, standard deviation and range) of all the studied calibration and validation sets are provided in Table 1. For PV, 10 calibration sets (C1′→C10′) and nine external validation sets (V2′→V10′) were selected. For example, set C2′ included 36 samples (66.7%) of coarse and fine sunflower tahini, whereas its complementary validation set V2′ included the remaining 18 commercial sunflower tahini samples (33.3%) of the factorial design. Calibration set C10′ (42 samples; 77.8%) and validation set V10′ (12 samples; 22.2%) were partly random selected, ensuring that both sets had a broad oxidation index range. Each validation set was composed of the samples not used for calibration. As Table 1 shows, four calibration sets (C1′→C4′) were selected for pAV, but no external validation sets were used for this oxidation index. For both PV and pAV, the same calibration and validation sets were used for both extracted fat phase (EFP) and the intact sunflower tahini (IST) spectra.

Different cross-validation strategies associated with the factors tested in the experiment (sample particle size, temperature and time) were used during calibration development when using the C1 calibration set. Cross-validation provides an assessment of calibration performance. The aim of this method is to keep a single sample (leave-one-out or full cross-validation) or a group of samples apart and develop a calibration with the remaining samples. The developed calibration is validated with the excluded samples, and the prediction values are recorded. This procedure is done consecutively until all the samples have been predicted once. The final calibration model is not tested. External validation sets were used for testing the final models.

The relative performance of the established partial least squares (PLS) models was assessed using the root mean square error of calibration (RMSEC), root mean square error of cross validation (RMSECV), root mean square error of prediction (RMSEP), standard error of calibration (SEC), standard error of cross-validation (SECV), standard error of prediction (SEP) and ratio of performance of deviation (RPD), as well as the correspondent coefficients of determination (R_{cal}^2, R_{cv}^2, R_p^2). RPD was computed as the ratio between standard deviation (SD) and SEP, and is related to the ability of the model to predict future data. RPD shows how good the calibration and prediction will work for analytical purposes. Cozzolino et al. [21] noted that a model with an RPD value greater than 3 is considered to be useful for screening and greater than 5 to be fit for quality control.

3. Results and discussion

3.1. Spectra description

Spectra were acquired for the EFP and the corresponding IST. Fig. 1 shows the mean spectra of an EFP and its IST: without pre-treatment (A); with SNV pre-treatment (B); with SNV pre-treatment, followed by the Savitzky-Golay first derivative 7 smoothing points and second polynomial order – d1 (7, 2) (C); and with SNV pre-treatment, followed by the Savitzky-Golay second derivative – d2 (9, 2) (D). The raw NIR spectrum of the EFP showed similarities with the IST spectrum for the NIR-specific absorption bands characteristic for oils, namely 1200 nm, 1400 nm, 1700–1780 nm, 2060–2200 nm and 2300–2380 nm [12]. These similarities were more apparent when SNV pre-treatment was performed. SNV is a widely used method that reduces spectral distortions due to scattering, treating each spectrum individually and independently. SNV centers and scales each spectrum individually, so that each has a mean of 0 and a standard deviation of 1 [31]. The 1600–1850 nm region showed two main bands in the vicinity of 1720 nm and 1758 nm for both EFP and IST. They are characteristics of the first overtone of the C–H stretching vibration of methyl, methylene and ethylene groups. Hourant et al. [32] stated that oils rich in

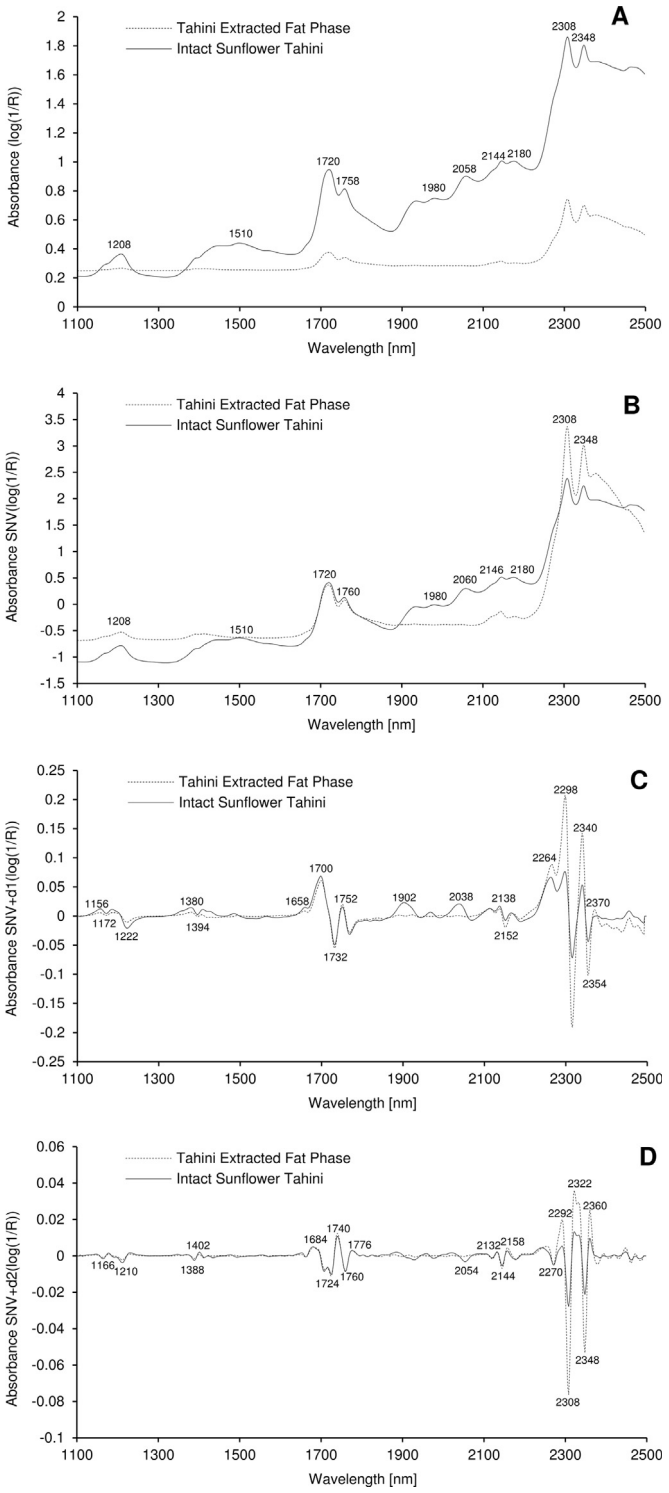

Fig. 1. Near-infrared mean spectra of intact tahini and extracted fat phase: (**A**) without pre-treatments; (**B**) standard normal variate (SNV) pre-treatment; (**C**) SNV followed by Savitzky-Golay first derivative - d1 (7, 2) pre-treatment; (**D**) SNV followed by Savitzky-Golay second derivative - d2 (9, 2) pre-treatment.

polyunsaturated fatty acids have a peak centered at a lower wavelength (1720–1722 nm) than oils rich in monounsaturated fatty acids (1724 nm) or fats rich in saturated fatty acids (1726 nm). As expected, both the EFP and IST spectra showed peaks around 1720 nm, confirming the high polyunsaturated fatty acid content characteristic of sunflower seeds. The last part of the EFP and the IST spectra contain two intense absorption bands centered near 2308 nm and 2348 nm, respectively. This part of the electromagnetic spectrum is characteristic of the combination of C–H stretching vibration with other vibrational modes. When the raw EFP and IST spectra are compared, the raw spectrum of extracted oil shows a horizontal baseline. In addition, to EFP, the IST spectrum showed absorption bands characteristic of proteins around 1510 nm, 1980 nm, 2050 nm and 2180 nm, which could be associated with the N-H stretching modes [33], confirming the high protein content (~21%) of sunflower tahini.

Agelet and Hurburgh [31] noted that the use of derivatives is another option for correcting the effect of overlapping bands (enhancing signal) and removing spectral base line offset (constant drift of the spectra base line intensity across wavelengths) and baseline slope (additive variation of the spectra base line intensity across wavelengths). A first-order derivative of log (1/R) resulted in a curve containing minima and maxima that corresponded to the point of inflection. It is rather difficult to visually interpret the first derivative because the derivative spectra did not follow the log (1/R) spectral pattern [34], as shown in Fig. 1A (log 1/R) compared with Fig. 1C (first derivative). This type of pretreatment is helpful in calibration development. Second-order derivative calculation results in a spectral pattern display of absorption bands and can be very helpful in spectral interpretation because, in this form, band intensity and band position are maintained with those in the log (1/R) spectral pattern [34]. The major advantage is band resolution enhancement, as shown in Fig. 1D. After the SNV and Savitzky-Golay second-derivative transformations, the EFP and IST absorption bands showed clear similarities with the absorption band position and intensity of oil and fats. The 1850–2050 nm region contained poor information for the characterization of oils and fats [32].

Log (1/R) increased with increasing particle size because the apparent path length became longer. The same sunflower tahini ground to different particle sizes therefore resulted in substantially different spectra (Fig. 2A). Osborne [35] stated that the effect is not additive, but multiplicative (*i.e.*, proportional to log [1/R]). In the reflectance spectra of food products, log (1/R) increased with increasing wavelength (Fig. 2A), and therefore the effect of particle size appeared to be a function of wavelengths [35]. Lima et al. [36] suggested that particle size distribution is more important than mean particle size, and if more than one mode is identified a mean value should not be used. With regard to the CVP, the samples could be classified as FinT < ComT < CoaT, ordered from finest to coarsest and including the industrial tahini. Correction for particle size could be accomplished empirically by multiple regression, but many spectroscopists prefer to use derivatives, multiplicative scatter correction (MSC) or SNV. The mean spectra for three different particle sizes of tahini samples after SNV pre-treatment and after SNV followed by the Savitzky-Golay second derivative pre-treatment were calculated. The offset baseline correction can be observed when preprocessing with SNV (Fig. 2B), whereas SNV followed by the second derivative shows a flat spectra baseline (Fig. 2C). Although the pre-processed spectra might look the same in the plots (Fig. 2C, 1100–2200 nm region), there were differences among absorbance intensities across wavelengths and these could be correlated with the compound of interest during the calibration stage.

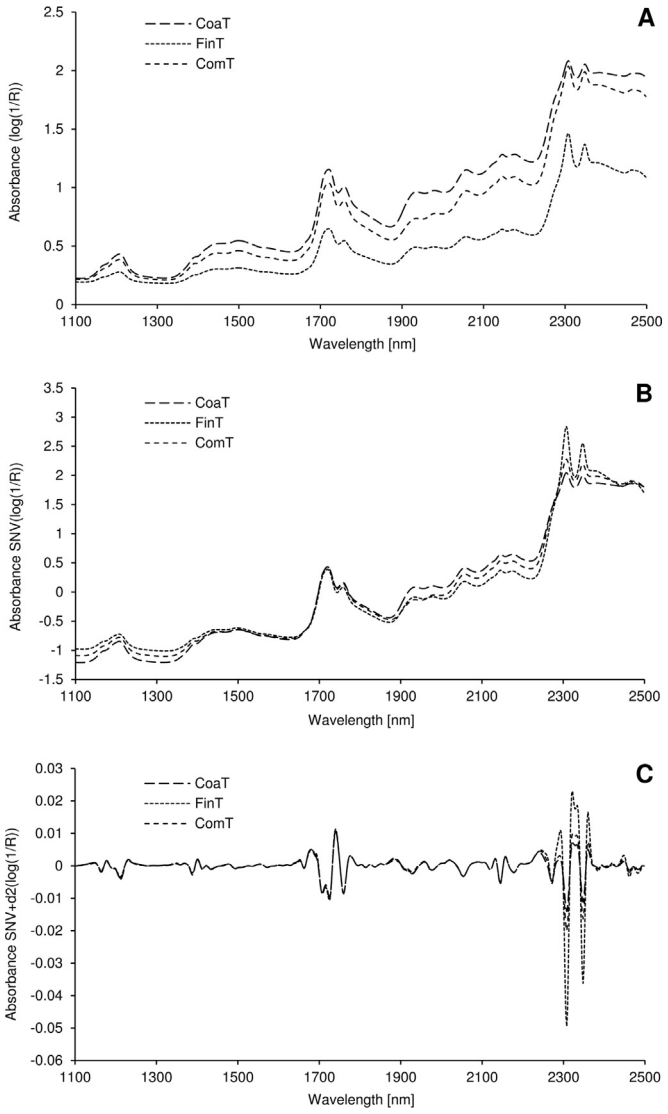

Fig. 2. Near-infrared mean spectra of intact tahini for different particle size samples: (**A**) without pre-treatments; (**B**) standard normal variate (SNV) pre-treatment; (**C**) SNV followed by Savitzky-Golay second derivative – d2 (9, 2) pre-treatment. Samples show trimodal particle size distribution with the following particle size populations: small (SP) [~0.2 to ~2 μm], middle (MP) [~2 to ~60 μm] and large (LP) [> ~60 μm]. Correspondent cumulative volume percentages of each size class CoaT (SP −9.61%, MP −43.03%, LP −47.36%); FinT (SP −16.67%, MP −55.03%, LP −28.30%) and ComT (SP −10.51%, MP −36.90%, LP −52.59%).

3.2. NIR and peroxide value

The PV of the samples analyzed ranged between 8.42 and 125.21 meq O_2 kg^{-1} fat. The highest PV value was about eight times higher than maximum allowable level for cold pressed and virgin vegetable oils [37]. A PV value of 100 meq O_2 kg^{-1} might not be very high, but animal studies have shown that this level of deteriorated fat and oil is neurotoxic [38]. Although 30 meq O_2 kg^{-1} is much less than 100 meq O_2 kg^{-1}, once the sudden oxidation starts during the propagation period the 100 meq O_2 kg^{-1} level is reached soon after the 30 meq O_2 kg^{-1} level [38]. Including these oxidized samples was essential to ensure the robustness of the NIR calibration models, even though their use in food is controversial. The lowest PV of sunflower tahini used was 8.42 meq O_2 kg^{-1}. This was similar to PVs reported in literature for freshly roasted sunflower seeds, 4.01–6.93 meq O_2 kg^{-1} after 5–15 min of microwave roasting [39], even though much smaller values (0.07 meq O_2 kg^{-1}) for the usual fresh sunflower oil have been

Table 2
Overview of PLS calibration models for PV, developed for calibration set C1′ (n=54 samples; n′= the size of the group of samples used in cross-validation; SD=23.88 meq O_2 kg^{-1}), EFP and IST spectra.

Product	Pre-processing	Spectral region [nm]	CV type[a]	n′/n	No. of factors	Calibration				Cross validation				
						R_{cal}^2	RMSEC	Slope	Bias	R_{cv}^2	RMSECV	Slope	Bias	RPD
EFP	None	1100–2500	Full	54/54	8	0.97	3.96	0.97	1.5E-04	0.94	5.68	0.94	2.4E-01	4.17
IST	None	1100–2500	Full	54/54	10	0.91	7.06	0.91	−1.1 E-04	0.72	12.65	0.79	3.3E-01	1.87
EFP	**SNV d1 (7, 2)**	**1140–1184; 1388–1440; 2026–2194**	**Full**	**54/54**	**3**	**0.97**	**3.45**	**0.97**	**−2.3 E-06**	**0.97**	**3.72**	**0.97**	**1.0E-02**	**6.36**
			Sample	18/54	3	0.97	3.45	0.97	−2.3 E-06	0.97	3.99	0.94	7.0E-02	5.94
			Temp	18/54	3	0.97	3.45	0.97	−2.3 E-06	0.97	3.69	0.98	1.2E-01	6.42
			Time	9/54	3	0.97	3.45	0.97	−2.3 E-06	0.97	3.68	0.96	−9.0E-02	6.42
IST	SNV d1 (7, 2)	1148–1180; 2064–2132	Full	54/54	6	0.97	3.78	0.97	−1.2 E-05	0.96	4.51	0.96	−2.0E-02	5.25
EFP	SNV d2 (9, 2)	1140–1184; 1388–1440; 2026–2194	Full	54/54	3	0.97	3.69	0.97	−1.1 E-05	0.97	4.12	0.95	−3.0E-02	5.74
IST	**SNV d2 (9, 2)**	**1148–1180; 2064–2132**	**Full**	**54/54**	**5**	**0.98**	**3.29**	**0.98**	**6.4 E-06**	**0.96**	**4.52**	**0.95**	**1.2E-01**	**5.23**
			Sample	18/54	8	0.98	2.54	0.98	3.3 E-06	0.92	7.54	0.89	3.2E+00	3.47
			Temp	18/54	6	0.98	3.01	0.98	6.5 E-06	0.96	5.01	0.89	−5.3E-01	4.75
			Time	9/54	5	0.98	3.29	0.98	6.4 E-06	0.96	4.97	0.95	−1.1E-01	4.76
EFP	MSC d1 (7, 2)	1140–1184; 1388–1440; 2026–2194	Full	54/54	3	0.97	3.45	0.97	-4.6 E-06	0.97	3.72	0.97	1.0E-02	6.35
IST	MSC d2 (9, 2)	1148–1180; 2064–2132	Full	54/54	5	0.98	3.26	0.98	9.2 E-06	0.96	4.32	0.95	7.0E-02	5.48
EFP	d1 (7, 2)	1140–1184; 1388–1440; 2026–2194	Full	54/54	4	0.97	3.51	0.97	-1.1 E-05	0.97	3.89	0.97	-1.0E-02	6.08
EFP	SNV d1 (7, 2)	1100–2200	Full	54/54	5	0.97	3.4	0.97	-1.2 E-05	0.96	4.23	0.96	6.0E-02	5.59
EFP	SNV d1 (7, 2)	2014–2194	Full	54/54	3	0.97	3.98	0.97	-2.9 E-06	0.96	4.28	0.96	-6.7E-03	5.53
IST	SNV d2 (9, 2)	1100–2200	Full	54/54	8	0.98	3.04	0.98	−4.6 E-06	0.95	4.91	0.93	-7.0E-02	4.82
IST	SNV d2 (9, 2)	2064–2132	Full	54/54	4	0.95	5	0.95	3.2 E-06	0.93	6.24	0.93	3.0E-02	3.79

EFP=extracted fat phase; IST=intact sunflower tahini; SNV=standard normal variate; MSC = multiple scattering correction; d1/ d2=first/second derivative; R_{cal}^2, R_{cv}^2=coefficients of determination for calibration and cross-validation; RMSEC=root mean square error of calibration; RMSECV=root mean square error of cross-validation; RPD=ratio of performance of deviation.

[a] Cross validation type: full or category options associated with the experimental design used: 3 (sample) × 3 (temperature) × 6 (time).

reported and used in calibration models [20]. An in-depth discussion of sunflower tahini PV changes during storage was recently published [40] in the context of assessing the influence of storage conditions and particle size on sunflower tahini colloidal and oxidative stability.

Calibration set C1′ (Table 1), which includes all 54 samples, was used in order to identify the best pre-treatment and the best NIR region when using a full cross-validation type for both EFP and IST. As shown in Table 2, the best PLS model result for EFP (calibration equation with three latent variables, RMSECV=3.72 meq O_2 kg^{-1} and RPD =6.36) was obtained when using SNV and the Savitzky-Golay first derivative in the 1140–1184 nm, 1388–1440 nm and 2026–2194 nm regions. The optimum number of PLS factors was determined by using the leave-one-out (full) cross validation procedure, plotting the RMSECV against the number of factors and searching for the minimum error (results not shown). MSC transformation of the EPF spectra gave similar results to SNV when followed by the first derivative. When the second derivative was used, higher RMSECVs (~4.12 meq O_2 kg^{-1}) were recorded in both cases. Similar results were obtained when the first derivative alone was applied (results not shown). When broader NIR regions (1100–2200/2500 nm) were included with or without treatment (SNV d1 (7, 2)), more latent variables were needed 5–8) in order to minimize RMSECV. If an excessive number of latent variables is included in the calibration, a fraction of noise is also modeled and the calibration becomes too specific to the calibration set. This phenomenon is known as over fitting, and it leads to a reduction in model accuracy in future predictions [31].

In the case of IST spectra without pre-treatment, and for the 1100–2500 nm region, a higher number of latent variables were required to build a model with an RMSECV of 12.65 meq O_2 kg^{-1}. Better results were acquired by optimizing the NIR regions used in calibration and pre-treating spectra. The best results were obtained when either MSC or SNV were followed by the Savitzky-Golay second derivative for the 1148–1180 nm and 2064–2132 nm regions. In these cases, the calibration model obtained had five latent variables, an RMSECV of 4.52 meq O_2 kg^{-1} and an RPD of 5.23.

The PV calibration for the EFP spectra (pre-treatment SNV d1 (7, 2); 1140–1184 nm, 1388–1440 nm and 2026–2194 nm regions) and the IST spectra (pre-treatment SNV d2 (9, 2); 1148–1180 nm and 2064–2132 nm regions) was considered suitable for quality control (RPD > 5). Plots of NIR predicted *vs.* reference data were linear and had slopes close to 1 (Fig. 3A and B).

The best NIR regions found for predicting PV in sunflower tahini were 1140–1184 nm 1388–1440 nm and 2026–2194 nm for EFP and 1148–1180 and 2064–2132 nm for IST. These regions were also important predictors of weighted regression coefficients (Fig. 4A and B). If the objective is to identify important predictors (wavelengths), the weighted regression coefficients plot should always be used if the data have been standardized. Wold et al. [41] noted that in the absence of knowledge about the relative importance of the variables, one of standard multivariate approaches is to scale each variable to unit variance by dividing them by their SDs. This corresponds to giving each variable (column) the same weight and prior importance in the analysis.

The best wavelengths for measuring PV in extracted oils and tahini can be interpreted in terms of chemical characteristics by

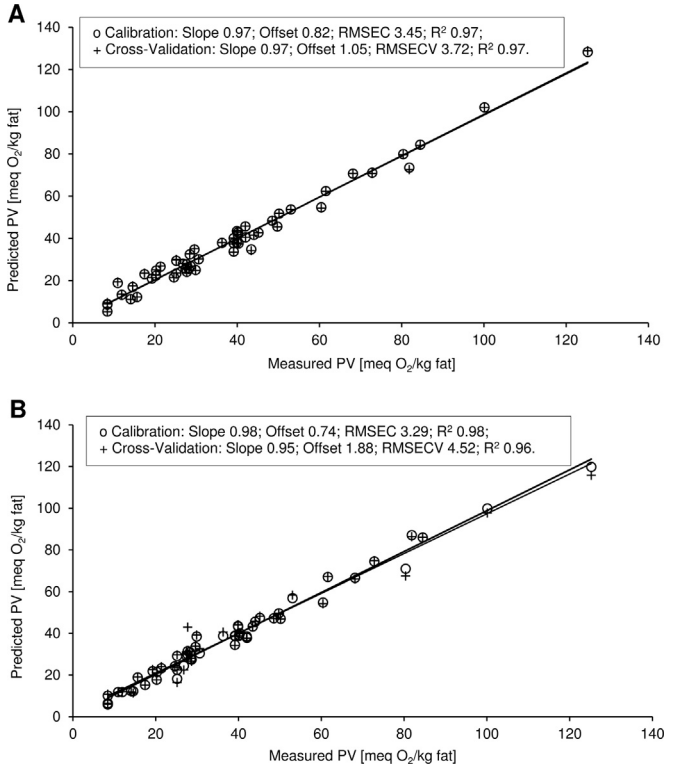

Fig. 3. NIR predicted values against measured data for PV-PLS calibration model (n=54 samples) for EFP based on three latent variables, using regions 1140–1184, 1388–1440 and 2026–2194 nm and SNV d1 (7, 2) (**A**) and for IST based on five latent variables, using regions 1148–1180, and 2064–2132 nm and SNV d2 (9, 2) (**B**).

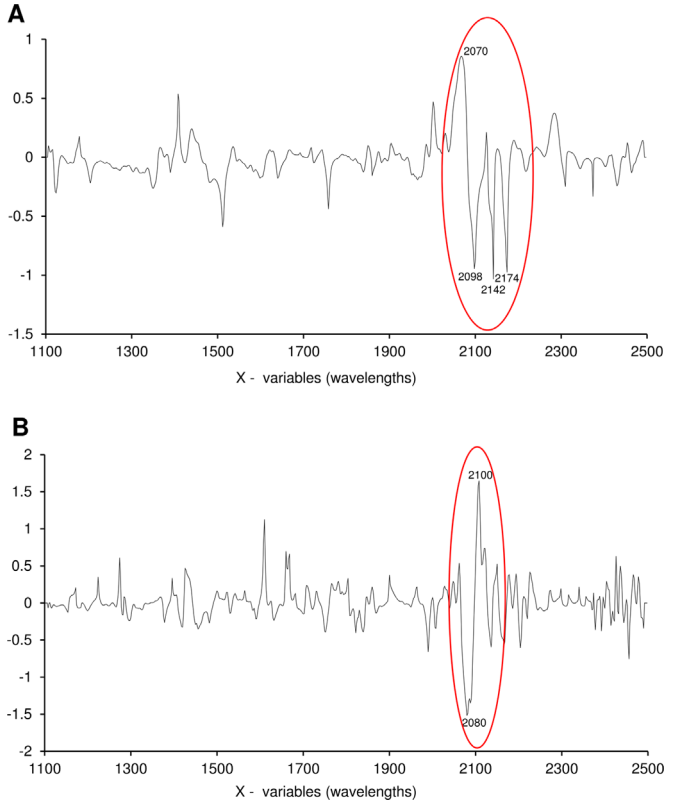

Fig. 4. Weighted Regression Coefficients for EFP standardized spectra 1100–2500 nm SNV d1 (7, 2) (**A**) and for IST standardized spectra 1100–2500 nm SNV d2 (9, 2) (**B**).

reference to previously known [34] chemical assignments. Absorptions around 1170 nm are caused by –HC=CH– structure with the C-H second overtone bond vibration, whereas 1410 nm probably represents the first overtones of O–H stretching vibrations [34]. The region around 2070–2090 nm appears to be highly significant for PV calibrations models of both EFP (Fig. 4A) and IST (Fig. 4B), this region being related to O–H combination according to Shenk et al. [34]. Similarly, Yildiz et al. [23] reported that 2084 nm was the key wavelength for lipid peroxide in the spectra of purified hydroperoxides of methyl oleate and methyl linoleate and could be used for determining lipid oxidation in edible oils.

Table 2 presents the PLS calibration statistics, with different cross-validation strategies linked to the factors tested in the experiment (sample granulometry, temperature and time), when using the best pre-processing techniques and NIR regions (marked in gray) selected for EFP and IST spectra. As can be seen from Table 2 when using EFP spectra, all the PLS calibration models that were developed, whatever the cross-validation strategy, gave similar results, the PLS model having three latent variables, R_{cv}^2 0.97, RMSECV between 3.68 and 3.99 meq O_2 kg^{-1} and good RPD values between 5.94 and 6.42. Where IST spectra were used, the worst result (eight PLS factors, R_{cv}^2 0.92, RMSECV 7.54 meq O_2 kg^{-1} and RPD 3.47) was obtained when cross-validation including sample type grouping was involved. This shows the importance of including a narrow range of particle size distribution samples in a calibration model when intending to measure the tahini PV of broader particle size samples using NIRS. For IST spectra, the other cross-validation strategies (full, time/temperature category) used for PLS calibration models gave similar results (five to six PLS factors included in the models; RPD 4.75-5.23) (Table 2). For IST spectra, however, only the calibration model using full cross-validation showed an RPD higher than 5.

In order to study the impact of the composition of the calibration and validation sets and to obtain a robust evaluation of the potential of using NIR to assess the oxidation status of tahini, for the sets described in Table 1, the best spectra pre-treatments and regions found previously for EFP and IST were used for developing the PLS calibration models. When using EFP spectra, the calibration models obtained (Table 3) for C2′-C10′ sets were based on three PLS factors (apart from set C4′, which was built on four latent variables) and had an R_{cal}^2 between 0.96 and 0.98, an RMSEC of 2.32–3.62 meq O_2 kg^{-1} and an RPD (data not shown) for full cross-validation of 4.61-7.6. The similar performance of developed EFP models indicated no influence of different groupings. When conducting an external validation with samples not used in the calibration models, however, lower RPD (3.21 and 3.46) and R_p^2(0.9 and 0.91) values were registered only for sets V7′ and V9′, respectively (Table 3), which are represented by all samples stored at 4 °C (V7′) and all samples from t3-t4 storage times (V9′). This can be explained only by smaller standard deviations of the V7′ and V9′ validation sets (Table 1), whereas the overall SEP (data not shown) of the V2′-V10′ sets ranged between 2.89 and 4.18 meq O_2 kg^{-1}, with the SEP of the V7′ and V9′ sets being included in this range. Generally, for the EFP spectra and excluding the V7′ and V9′ sets, the external validation worked well, with an RMSEP of 3.3–4.28 meq O_2 kg^{-1}, an R_p^2 of 0.94-0.98 and an RPD of 4.66-8.23.

For the IST spectra, however, different sample groupings (C2′-C10′) gave satisfactory results for cross-validation, but in the external validation test the results were unsatisfactory when the samples used were not the same type as those when the calibration model had been set up (*i.e.*, C4′, C5′, C7 and C9′). For the IST spectra, the developed PLS calibration models (Table 3) were based on three to five PLS factors, an R_{cal}^2 of 0.92-0.98 and an RMSEC of 2.72–4.78 meq O_2 kg^{-1}. For the same models cross-validation worked well, with sets C2′, C4′, C8′, C9′ and C10′ showing

Table 3
Statistics of PLS calibration and external validation for PV of EFP and IST spectra using different calibration and validation sets.

Product/calibration characteristics	Calibration						External validation					
	CS	No. of factors	R_{cal}^2	RMSEC	Slope	Bias	VS	R_p^2	RMSEP	Slope	Bias	RPD
EXTRACTED FAT PHASE SNV d1 (7, 2); 1140–1184; 1388–1440; 2026–2194 nm	**C2′**	3	0.98	3.12	0.98	-7.1E-06	**V2′**	0.94	4.28	0.87	1.4E+00	4.66
	C3′	3	0.96	3.62	0.96	3.4 E-07	**V3′**	0.96	4.25	1.04	-3.0E+00	7.09
	C4′	3	0.98	3.47	0.98	-6.1 E-06	**V4′**	0.97	3.36	1.01	1.9E+00	7.21
	C5′	4	0.97	2.32	0.97	5.7 E-06	**V5′**	0.98	3.86	1.04	3.1E-01	8.23
	C6′	3	0.98	3.46	0.98	8.7 E-07	**V6′**	0.95	3.3	0.91	3.5E-01	4.97
	C7′	3	0.98	3.33	0.98	4.6 E-06	**V7′**	0.90	3.89	0.89	-3.4E-01	3.21
	C8′	3	0.97	3.56	0.97	6.6 E-07	**V8′**	0.97	3.42	0.91	3.6E-01	6.23
	C9′	3	0.98	3.1	0.98	5.9 E-06	**V9′**	0.91	4.07	0.94	-4.6E-01	3.46
	C10′	3	0.98	3.35	0.98	1.6 E-05	**V10′**	0.95	3.55	0.97	-1.5E-01	4.98
INTACT SUNFLOWER TAHINI SNV d2 (9, 2); 1148–1180; 2064–2132 nm	**C2′**	5	0.98	2.97	0.98	5.2 E-08	**V2′**	0.92	5.14	1.11	3.8E+00	5.51
	C3′	5	0.97	3.25	0.97	-1.2 E-05	**V3′**	0.85	8.3	0.89	-7.4E+00	5.67
	C4′	4	0.98	3.18	0.98	6. 6E-07	**V4′**	0.34	27.81	0.8	1.6E+01	0.89
	C5′[a]	4	0.92	4.08	0.92	-3.1 E-06	**V5′**	0.76	15.22	0.64	-9.4E+00	2.65
	C6′[a]	5	0.96	4.78	0.96	1.1 E-05	**V6′**	0.91	4.78	1.01	-1.2E+00	3.53
	C7′[a]	3	0.96	4.74	0.96	-2.6 E-06	**V7′**	0.45	9.21	1.25	4.5E+00	1.55
	C8′	5	0.98	2.94	0.98	1.3 E-05	**V8′**	0.93	5.37	1.01	-1.1E+00	4.03
	C9′	5	0.98	2.72	0.98	2.4 E-06	**V9′**	0.71	7.47	1.01	3.4E+00	2.10
	C10′	5	0.98	2.96	0.98	-4.1 E-06	**V10′**	0.91	5.1	0.79	2.0E-02	3.47

CS=calibration set; VS=validation set; RMSEP=root mean square error of prediction; Rp2=coefficients of determination for prediction; other abbreviations are as in Table 2.

[a] Region 1148–1180 nm was excluded.

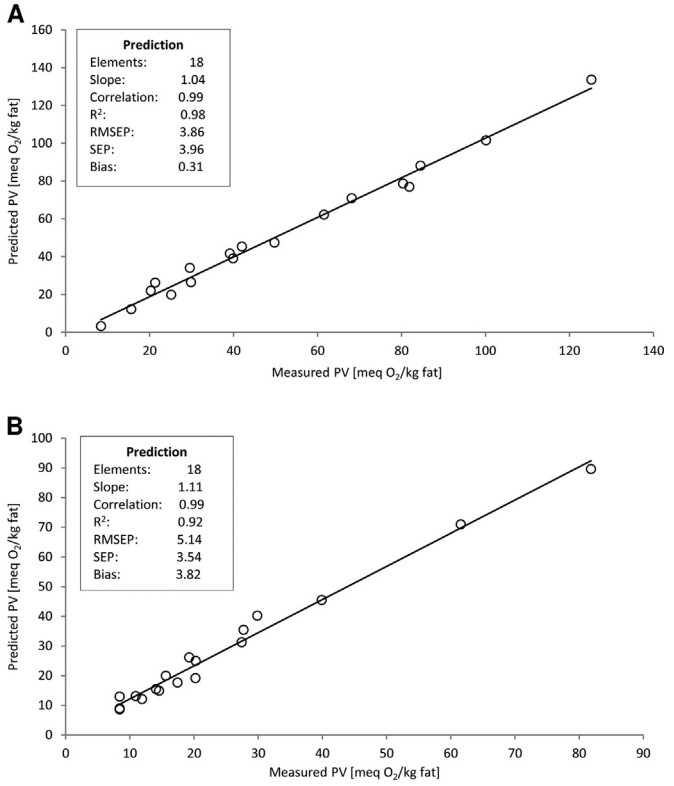

Fig. 5. Scatter plot diagram comparing NIR predicted and measured PV of the V5 validation set (n=18) for EFP (**A**) and the V2 validation set for IST (**B**). Ordinate values are the predicted PV values from EFP (**A**) or IST (**B**) NIR spectra, respectively. Abscissa values are PV as determined by reference method.

RPD values higher than 5 (results not shown). For external validation, sets V2′ and V3′ gave RPD values higher than 5. This shows that the PLS model based on the extreme particle size sunflower tahini prototypes gave good predictions of the PV of commercial sunflower tahini. Similarly, the PLS model built with the coarsest particle size of the sunflower tahini prototype and commercial tahini gave good predictions of the finest size of the sunflower tahini sample (Table 3). The measured *vs.* predicted scatter plots for the best external validations, are shown for both EFP (Fig. 5A) and IST (Fig. 5B).

3.3. NIR and p-anisidine value

The pAVs of the samples analyzed ranged between 3.78 and 8.9 (pAVs have no dimensions, and are calculated and quoted on the basis of 1 g of the test sample in 100 ml of a mixture of solvent and reagent). The impact on sunflower tahini pAVs of storage conditions and sample particle size was discussed in a recently published work [40]. According to Man et al. [42], as a rule of thumb the pAV should be less than 10 for good quality oil. The pAV of the analyzed samples in our study were below this threshold. When evaluating the oxidative status of food products, however, both primary and secondary oxidation indices should be assessed. There were poor correlations between NIR-predicted values and the reference data of pAVs for both EFP and IST, whatever calibration sample sets (Table 1), pre-treatments or regions used. During the construction of pAV PLS calibration models using IST and EFP spectra and for calibration set C1″, different pre-treatments and/or NIR regions were tested in order to improve the RMSEC, RMSECV and correspondent coefficients of determination (Table 4). None of the evaluated pre-treatments resulted in an acceptable RPD, indicating that the prediction of the pAVs for EFP and IST, using NIR, could not be achieved in our experiment. Cozzolino et al. [21] also reported negative results when developing calibration models for the pAV of fish oils. Yildiz et al. [23] noted that the chances of measuring soybean oil pAVs using NIR were limited, especially when using an external validation set. The same authors concluded that although developing successful pAV calibrations for narrowly defined sample sets might be possible, global calibrations applicable to a wide range of samples could be more difficult to achieve. The SEP values (0.59-0.92) obtained in the latter study were still relatively large compared with the standard deviation of pAVs in the sample set (SD=0.91). Szabó et al. [43] concluded, however, that using NIR to estimates pAVs does meet practical requirements when the lipid fractions of rapeseed, sunflower, pig and goose fat are involved, but the robustness of the PLS models based on RPD value was not assessed. When computing the RPDs from their results, there were doubts about the robustness of the pAV PLS models, whereas the RPDs for rapeseed oil, sunflower oil, pig fat and goose fat calibrations were 1.45, 1.01, 1.89, and 2.73, respectively. Szabó et al. [44] also reported good results based on calibration and cross-validation results (SEC =11.782; R_{cal}^2=0.912; SECV =19.435; R_{cv}^2=0.772) when using NIR for predicting pAV in lard during prolonged

Table 4
Overview of PLS calibration models for pAV developed for calibration set C1″ (n=54 samples; SD =1.32), EFP and IST spectra.

Product	Pre-processing	Spectral region [nm]	No. of factors	Calibration				Cross validation[a]				
				R_{cal}^2	RMSEC	Slope	Bias	R_{cv}^2	RMSECV	Slope	Bias	RPD
EFP	None	1100–2500	8	0.57	0.85	0.57	1.3 E-05	0.19	1.19	0.41	2.0E-02	1.09
EFP	None	1100–2200	7	0.49	0.93	0.49	-2.5 E-06	0.19	1.2	0.35	1.0E-02	1.09
IST	None	1100–2500	10	0.8	0.58	0.8	-2.5 E-06	0.25	1.15	0.54	3.0E-02	1.14
IST	None	1100–2200	10	0.8	0.58	0.8	7.1 E-07	0.62	0.81	0.72	-1.0E-02	1.61
EFP	SNV	1100–2500	7	0.56	0.86	0.56	5.3 E-06	0.2	1.19	0.41	2.0E-02	1.10
IST	SNV	1100–2500	10	0.85	0.49	0.85	7.1 E-06	0.33	1.09	0.56	3.0E-02	1.20
EFP	SNV d1 (7, 2)	1100–2500	5	0.57	0.85	0.57	-2.1 E-06	0.37	1.05	0.46	2.0E-02	1.25
IST	SNV d1 (7, 2)	1100–2500	10	0.95	0.28	0.95	1.8 E-07	0.61	0.83	0.69	1.0E-02	1.57
EFP	SNV d2 (9, 2)	1100–2500	4	0.51	0.91	0.51	-9.7 E-08	0.25	1.15	0.31	2.0E-02	1.14
IST	SNV d2 (9, 2)	1100–2500 1388–1430	10	0.94	0.31	0.94	1.3 E-06	0.57	0.87	0.64	7.7E-05	1.50
EFP	SNV d2 (9, 2)	1720–1770 2114–2154 1402–1462	6	0.68	0.73	0.68	-1.1 E-06	0.53	0.91	0.6	2.0E-02	1.43
IST	SNV d2 (9, 2)	1654–1726 1888–2204	8	0.9	0.4	0.9	1.4E-06	0.76	0.64	0.8	-1.0E-02	2.06

Abbreviations are as in Table 2.

[a] Full cross-validation.

heating under 200 °C and using a 2000–2500 nm wavelength interval, but the obtained models were not tested by an external validation and no RPD values were provided. Yildiz et al. [23] considered that NIR correlations for pAVs are probably secondary correlations, rather than the direct measurements of carbonyl compounds, making pAV prediction using NIR spectroscopy problematic. It is well known that the pAV test measures unsaturated aldehydes mainly and is particularly sensitive to conjugated aldehydes, especially dienals [30]. Szabó et al. [43] reported that the molar absorption of the reaction products of p-anisidine and different aldehydes showed several magnitude differences (*e.g.*, *n*-hexanal 500; 2-heptenal 60,00; 2,4-decadienal 20,000 at 350 nm). The poor results of the pAV PLS models for both EFP and IST NIR spectra in our study, therefore, could be explained by the fact that the pAV reference method is an indirect measure of carbonyl compounds in general and its overall response is a function of the types of aldehydes present. In addition, during the oxidation of tahini the actual amounts of various aldehyde types formed are unknown, although chemical pAV determination does give a general indication of the total amount of carbonyl compounds in the oil.

4. Conclusion

The oxidation status of sunflower tahini - a heterogeneous food model representative of the oilseed-based products category - changes during storage, and the need to measure this status quickly and accurately in order to ensure the safety of the product for consumption prompted us to search for a rapid, easy and cost-effective analytical method. In addition, it was important that the analysis could be performed for the product as it is ("*in situ*") in order to avoid a prior extraction of the fat phase, which determines supplementary human and material costs and can be the source of erroneous results. Moreover, this fact will allow future method's optimization for a rapid "on-line" *in situ* determination of the product's PV and pAV. Our study therefore sought to develop multivariate calibration models that could predict PVs and pAVs in sunflower tahini *in situ* using NIR spectroscopy. The analytical performance of the new methods developed here was determined, including matrix effects (particle size distribution) and storage conditions (temperature and time), the methods being validated by comparison with standard methods.

The NIR spectra measured for the EFP were similar to the IST spectra for the NIR-specific absorption bands characteristic of oils, these similarities being more apparent when SNV or SNV and Savitzky-Golay second-derivative pre-treatments were performed. In addition, to EFP, the IST spectrum showed absorption bands characteristic of proteins, confirming the high protein content of sunflower tahini. The same sunflower tahini ground to different particle sizes resulted in substantially different spectra, whereas the Log (1/R) increased with increasing particle size, because the apparent path length became longer. The correction of particle size effects was performed by SNV or SNV followed by the Savitzky-Golay second derivative pre-treatments.

The best PV calibration models for EFP spectra and IST spectra were considered good for quality control (RPD >5). The best PV PLS model result for EFP (RPD 6.36) was obtained when using SNV and the Savitzky-Golay first derivative in the 1140–1184 nm, 1388–1440 nm and 2026–2194 nm regions. In the case of IST spectra, the best PV models (RPD 5.23) were obtained when either MSC or SNV were followed by the Savitzky-Golay second derivative for the 1148–1180 nm and 2064–2132 nm regions. When using EFP spectra, all the PV PLS calibration models, whatever the cross-validation strategy, gave similar results, whereas for IST spectra the worst result was obtained when a cross-validation including sample type grouping was involved, showing the importance of including a narrow range of particle size distribution samples in calibration models when measuring the tahini PV of broader particle size samples using NIRS. For the EFP and IST spectra, apart from when samples used in external validation were not in the same particle size range as those samples used for the calibration model set-up, the external validation worked well, the best PV-PLS calibration models being considered suitable for quality control.

Using NIR to predict the pAV for EFP and IST seems more problematic. The performance of the calibration models developed fell below the minimum requirements, whatever calibration sample sets, pre-treatments or regions were used.

The results obtained in this study will facilitate the development of future NIR calibration models for the *in situ* analytical measurement of the oxidative status of similar products, including sesame tahini, hazelnut and cocoa liquor used for chocolate production, peanut butter, and hazelnut, almond and pistachio spreads, demonstrated thus their analytical applicability. It was shown a substantial advantage over existing methods, the analysis proposed here being performed on sunflower kernel tahini which was considered a good example of a complex food matrix showing no alterations treatments (drying, extraction, centrifugation, evaporation, *etc.*).

In the development of robust NIR PLS models for analytically measuring the oxidative stability of oilseed-based food products, we recommend that suitable calibration sets containing samples of different particle sizes stored at different temperatures should be selected. In addition, characterizing sunflower tahini and providing an NIR analytical method for the rapid assessment of its oxidative stability will facilitate the superior valorization of sunflower kernels as an allergen-free alternative to more expensive hazelnut, almond, pistachio, sesame, peanut and cocoa pastes.

Acknowledgements

The authors wish to thank Mrs Anne Mouteau and Mrs Marianne Flahaux from the Valorisation of Agricultural Products Department, Walloon Agricultural Research Centre (CRA-W), Gembloux, Belgium for their technical support. They would also like to thank Mrs Kay Powell (CGLS, Belgium) and Mr Tyson Buerkle, Eng. (Cornell University, Natural Resources Alumni) for reviewing this manuscript from an English language perspective. This paper was published within the framework of the European Social Fund (Human Resources Development Operational Programme 2007–2013, project no. POSDRU/159/1.5/S/132765).

References

[1] B. Barriuso, I. Astiasarán, D. Ansorena, A review of analytical methods measuring lipid oxidation status in foods: a challenging task, Eur. Food Res. Technol. 236 (2013) 1–15.
[2] R. Karoui, G. Downey, C. Blecker, Mid-infrared spectroscopy coupled with chemometrics: A tool for the analysis of intact food systems and the exploration of their molecular structure – quality relationships – A review, Chem. Rev. 110 (2010) 6144–6168.
[3] B. Škrbić, B. Filipčev, Nutritional and sensory evaluation of wheat breads supplemented with oleic-rich sunflower seed, Food Chem. 108 (2008) 119–129.
[4] I.M. Lima, H.S. Guraya, Optimization analysis of sunflower butter, J. Food Sci. 70 (2005) 365–370.
[5] V. Mureşan, C. Blecker, S. Danthine, E. Racolţa, S. Muste, Confectionery products (halva type) obtained from sunflower: production technology and quality alterations. A review, Revue Biotechnol. Agron., Société Environ. 17 (2013) 651–659.
[6] G. Muttagi, N. Joshi, Y.G. Shadakshari, R. Chandru, Storage stability of value added products from sunflower kernels, J. Food Sci. Technol. 51 (2014) 1806–1816.
[7] S. González-Pérez, J.M. Vereijken, Sunflower proteins: overview of their physicochemical, structural and functional properties, J. Sci. Food Agric. 87 (2007)

2173–2191.
[8] M.C. Dobarganes, J. Velasco, Analysis of lipid hydroperoxides, Eur. J. Lipid Sci. Technol. 104 (2002) 420–428.
[9] A.A. Kaddour, E. Grand, N. Barouh, B. Baréa, P. Villeneuve, B. Cuq, Near-infrared spectroscopy for the determination of lipid oxidation in cereal food products, Eur. J. Lipid Sci. Technol. 108 (2006) 1037–1046.
[10] Y. Ni, M. Mei, S. Kokot, Analysis of complex, processed substances with the use of NIR spectroscopy and chemometrics: classification and prediction of properties — the potato crisps example, Chemom. Intell. Lab. Syst. 105 (2011) 147–156.
[11] I.N. Hayati, Y.B.C. Man, C.P. Tan, I.N. Aini, Monitoring peroxide value in oxidized emulsions by Fourier transform infrared spectroscopy, Eur. J. Lipid Sci. Technol. 107 (2005) 886–895.
[12] D. Givens, J.D. Boever, E. Deaville, The principles, practices and some future applications of near infrared spectroscopy for predicting the nutritive value of foods for animals and humans, Nutr. Res. Rev. 10 (1997) 83–114.
[13] J.A. Cayuela, Md.C.P. Camino, , Prediction of quality of intact olives by near infrared spectroscopy, Eur. J. Lipid Sci. Technol. 112 (2010) 1209–1217.
[14] O. Niewitetzki, P. Tillmann, H.C. Becker, C. Möllers, A new near-infrared reflectance spectroscopy method for high-throughput analysis of oleic acid and linolenic acid content of single seeds in oilseed rape (Brassica napus L.), J. Agric. Food Chem. 58 (2009) 94–100.
[15] T. Sato, A. Maw, M. Katsuta, NIR reflectance spectroscopic analysis of the FA composition in sesame (Sesamum indicum L.) seeds, J. Am. Oil Chem. Soc. 80 (2003) 1157–1161.
[16] A. Fassio, D. Cozzolino, Non-destructive prediction of chemical composition in sunflower seeds by near infrared spectroscopy, Ind. Crop. Prod. 20 (2004) 321–329.
[17] S. Rudolphi, H. Becker, A. Schierholt, S. von Witzke-Ehbrecht, Improved estimation of oil, linoleic and oleic acid and seed hull fractions in safflower by NIRS, J. Am. Oil Chem. Soc. 89 (2012) 363–369.
[18] Ma.D. Guillén, N. Cabo, Fourier transform infrared spectra data *versus* peroxide and anisidine values to determine oxidative stability of edible oils, Food Chem. 77 (2002) 503–510.
[19] F.R. van de Voort, A.A. Ismail, J. Sedman, J. Dubois, T. Nicodemo, The determination of peroxide value by fourier transform infrared spectroscopy, J. Am. Oil Chem. Soc. 71 (1994) 921–926.
[20] S. Armenta, S. Garrigues, M. de la Guardia, Determination of edible oil parameters by near infrared spectrometry, Anal. Chim. Acta 596 (2007) 330–337.
[21] D. Cozzolino, I. Murray, A. Chree, J.R. Scaife, Multivariate determination of free fatty acids and moisture in fish oils by partial least-squares regression and near-infrared spectroscopy, LWT – Food Sci. Technol. 38 (2005) 821–828.
[22] M.H. Moh, Y.B. Che Man, F.R. van de Voort, W.J.W. Abdullah, Determination of peroxide value in thermally oxidized crude palm oil by near infrared spectroscopy, J. Am. Oil Chem. Soc. 76 (1999) 19–23.
[23] G. Yildiz, R. Wehling, S. Cuppett, Method for determining oxidation of vegetable oils by near-infrared spectroscopy, J. Am. Oil Chem. Soc. 78 (2001) 495–502.
[24] M. Allendorf, A. Subramanian, L. Rodriguez-Saona, Application of a handheld portable mid-infrared sensor for monitoring oil oxidative stability, J. Am. Oil Chem. Soc. 89 (2011) 79–88.
[25] E. Birkel, L. Rodriguez-Saona, Application of a portable handheld infrared spectrometer for quantitation of trans fat in edible oils, J. Am. Oil Chem. Soc. 88 (2011) 1477–1483.
[26] C.A. Nunes, Vibrational spectroscopy and chemometrics to assess authenticity, adulteration and intrinsic quality parameters of edible oils and fats, Food Res. Int. 60 (2014) 255–261.
[27] V. Muresan, S. Danthine, E. Racolta, S. Muste, C. Blecker, The influence of particle size distribution on sunflower tahini rheology and structure, J. Food Process Eng. (2014) 411–426.
[28] J. Folch, M. Lees, G. Sloane-Stanley, A simple method for the isolation and purification of total lipids from animal tissues, J. Biol. Chem. 226 (1957) 497–509.
[29] T. Crowe, P. White, Adaptation of the AOCS official method for measuring hydroperoxides from small-scale oil samples, J. Am. Oil Chem. Soc. 78 (2001) 1267–1269.
[30] AOCS, Method Cd 18-90 p-Anisidine value, Official Methods of Analysis of the American Oil Chemists Society, 1997.
[31] L.E. Agelet, C.R. Hurburgh, A tutorial on near infrared spectroscopy and its calibration, Crit. Rev. Anal. Chem. 40 (2010) 246–260.
[32] P. Hourant, V. Baeten, M.T. Morales, M. Meurens, R. Aparicio, Oil and fat classification by selected bands of near-infrared spectroscopy, Appl. Spectrosc. 54 (2000) 1168–1174.
[33] V. Svensson, Handling Complex Data in Food Analysis – A Chemometric Approach, PhD Thesis, Faculty of Life Sciences, University of Copenhagen, Copenhagen, Denmark, 2008.
[34] J.S. Shenk, M.O. Westerhaus, J.J. Workman, Application of NIR spectroscopy to agricultural products, in: D.A. Burns, E.W. Ciurczak (Eds.), Handbook of Near-Infrared Analysis, 3rd ed,CRC Press, 2007, pp. 347–386.
[35] B.G. Osborne, Near-Infrared Spectroscopy in Food Analysis, Encyclopedia of Analytical Chemistry, John Wiley & Sons, Ltd, 2006.
[36] I.M. Lima, H.S. Guraya, E.T. Champagne, Improved peanut flour for a reduced-fat peanut butter product, J. Food Sci. 65 (2000) 854–861.
[37] FAO, Codex Standard for Named Vegetable Oils, Codex Stan 210: 1-16, CODEX ALIMENTARIUS, 1999.
[38] N. Gotoh, S. Wada, The importance of peroxide value in assessing food quality and food safety, J. Am. Oil Chem. Soc. 83 (2006) 473–474.
[39] F. Anjum, F. Anwar, A. Jamil, M. Iqbal, Microwave roasting effects on the physico-chemical composition and oxidative stability of sunflower seed oil, J. Am. Oil Chem. Soc. 83 (2006) 777–784.
[40] V. Mureşan, S. Danthine, S. Bolboacă, E. Racolţa, S. Muste, C. Socaciu, C. Blecker, Roasted Sunflower kernel paste (tahini) stability: Storage conditions and particle size influence, J. Am. Oil Chem. Soc. 92 (2015) 669–683.
[41] S. Wold, M. Sjöström, L. Eriksson, PLS-regression: a basic tool of chemometrics, Chemom. Intell. Lab. Syst. 58 (2001) 109–130.
[42] Y.B.C. Man, J.L. Liu, B. Jamilah, R.A. Rahman, Quality changes of refined-bleached-deodorized (RBD) palm olein, soybean oil and their blends during deep-fat frying, J. Food Lipids 6 (1999) 181–193.
[43] A. Szabó, G. Bázár, L. Locsmándi, R. Romvári, Quality alterations of four frying fats during long-term heating (conventional analysis and NIRS calibration), J. Food Qual. 33 (2010) 42–58.
[44] A. Szabó, G. Bázár, G. Andrássy-Baka, L. Locsmándi, R. Romvári, A near infrared spectroscopic (NIR) approach to estimate quality alterations during prolonged heating of lard, Acta Aliment. 38 (2009) 97–106.